J. Cell. Mol. Med. Vol 19, No 3, 2015 pp. 642-650

Impact of phosphomimetic and non-phosphorylatable mutations of phospholemman on L-type calcium channels gating in HEK 293T cells

Kai Guo #, Yue-Peng Wang #, Zhi-Wen Zhou, Yi-Bo Jiang, Wei Li, Xiao-Meng Chen, Yi-Gang Li *

Department of Cardiology, Xin Hua Hospital Affiliated to Shanghai Jiao Tong University School of Medicine, Shanghai, China

Received: June 7, 2014; Accepted: October 10, 2014

Abstract

Background: Phospholemman (PLM) is an important phosphorylation substrate for protein kinases A and C in the heart. Until now, the association between PLM phosphorylation status and L-type calcium channels (LTCCs) gating has not been fully understood. We investigated the kinetics of LTCCs in HEK 293T cells expressing phosphomimetic or nonphosphorylatable PLM mutants. **Methods**: The LTCCs gating was measured in HEK 293T cells transfected with LTCC and wild-type (WT) PLM, phosphomimetic or nonphosphorylatable PLM mutants: 6263AA, 6869AA, AAAA, 6263DD, 6869DD or DDDD. **Results**: WT PLM significantly slowed LTCCs activation and deactivation while enhanced voltage-dependent inactivation (VDI). PLM mutants 6869DD and DDDD significantly increased the peak of the currents. 6263DD accelerated channel activation, while 6263AA slowed it more than WT PLM. 6869DD significantly enhanced PLM-induced increase of VDI. AAAA slowed the channel activation more than 6263AA, and DDDD accelerated the channel VDI more than 6869DD. **Conclusions**: Our results demonstrate that phosphomimetic PLM could stimulate LTCCs and alter their dynamics, while PLM nonphosphorylatable mutant produced the opposite effects.

Keywords: phospholemman • phosphorylation sites mutation • L-type calcium channels • activation • voltage-dependent inactivation • deactivation

Introduction

Phospholemman (PLM), a member of the FXYD gene family of small ion transport regulators [1], is abundantly expressed in the cardiac sarcolemma and can modulate Na^+-K^+-ATPase (NKA) [2–4] and Na^+/Ca^{2+} exchanger (NCX) [5–7]. Previous studies demonstrated that PLM coimmunoprecipitated LTCCs ($Ca_V1.2$ channels) [8] and modulated the important gating process of $Ca_V1.2$ channels [8, 9]. PLM is also a major sarcolemmal substrate for protein kinases A (PKA) and C (PKC) in the myocardium [10, 11]. When phosphorylated at serine^{68}, PLM can stimulate NKA [2, 3, 12] and inhibit NCX [5, 7] in cardiac myocytes. As the activity status of LTCCs is related to the risk of various malignant arrhythmias, such as timothy syndrome (TS) [13–16], modulating PLM phosphorylation might be a potential strategy for preventing and treating arrhythmias. The role of PLM phosphorylation in the regulation of $Ca_V1.2$ gating kinetics remains to be elucidated. In this study, we examined the impact of PLM phosphorylation status on $Ca_V1.2$ gating kinetics in HEK 293T cells using site-directed mutagenesis and whole-cell patch-clamp electrophysiology techniques.

Materials and methods

Construction of WT and mutant PLM

The coding sequence of human PLM was amplified by polymerase chain reaction (PCR) with a His tag on C-terminus, digested with NheI and NotI, and inserted into pCDNA3.1(+)-IRES-GFP vector using the same restriction sites. PLM mutants, 6263AA, 6869AA, AAAA, 6263DD, 6869DD and DDDD, were constructed by PCR-based site-directed mutagenesis (Table S1 shows primers used to introduce the desired mutations into PLM at positions corresponding to amino acids 62, 63, 68

#Contributed equally.
*Correspondence to: Professor Dr. Med. Yi-Gang LI,
Department of Cardiology, Xin Hua Hospital Affiliated to
Shanghai Jiao Tong University School of Medicine,
1665 Kongjiang Road, Shanghai 200092, China.
Tel.: +862125078999-7265
Fax: +862165083740
E-mail: drliyigang@outlook.com

doi: 10.1111/jcmm.12484

and 69). WT PLM and mutants were confirmed by qualitative restriction map analysis, DNA sequence analysis and Western blot analysis.

Cell culture and transfection

HEK 293T cells from ATCC (Manassas, VA, USA) were cultured at 37°C and 5%CO_2 in DMEM-F12 medium (Gibco, CA, USA) supplemented with 10% foetal bovine serum and 1% penicillin-streptomycin. HEK 293T cells were transiently transfected with Hilymax following the manufacturer's instructions (Dojindo Laboratories, Kumamoto, Japan). cDNAs encoding $Ca_V1.2$ (α_1C subunit of LTCCs) [17], the auxiliary subunits, $\alpha_2\delta$ [18] and β_1b [19] (all subcloned into pCDNA3.1) were cotransfected with either empty vector (EV), WT PLM or mutant PLMs at equal molar ratios.

Electrophysiology

Whole-cell patch-clamp recordings were performed as described previously [8, 9]. Briefly, whole-cell currents were recorded at room temperature within 24–48 hrs post-transfection. Pipettes were pulled from borosilicate glass (1B150F-3, World Precision Instruments, Sarasota, FL, USA) using a Narishige PC-10 micropipette puller (Narishige, Japan). The pipette resistance ranged from 3.0 to 4.0 MΩ when the pipette was filled with the internal solution. Ionic currents were recorded in a bath solution containing 130 mM *N*-methyl-D-glucamine (NMG)-aspartate, 10 mM HEPES, 10 mM 4-aminopyridine, 10 mM glucose, 1 mM $MgCl_2$ and 10 mM $BaCl_2$. The internal solution contained 140 mM NMG-$MeSO_3$, 10 mM EGTA, 1 mM $MgCl_2$, 4 mM Mg-ATP and 10 mM HEPES. The osmolarity was adjusted to 300 mmol/kg with dextrose, and the pH was adjusted to 7.35. The use of Na^+, K^+ and Ca^{2+} free solutions enabled the recording of isolated $Ca_V1.2$ currents by eliminating possible contamination from currents originating from the NKA and NCX. The data were acquired using a HEKA EPC10 amplifier and PULSE/PULSEFIT software (ALA Scientific Instruments, Farmingdale, NY, USA). Leak and capacitive transients were corrected by P/4 leak subtraction. The series resistance was typically <8 MΩ and compensated at 70%. The tail currents were sampled at 50 kHz and filtered at 5.0 kHz. All other currents were sampled at 20 kHz and filtered at 3.0 kHz.

Data analysis

The data were analysed using Fitmaster (ALA Scientific Instruments) and Origin (Originlab, Northampton, MA, USA) software. A one-way ANOVA was used to evaluate the statistical significance. All data were presented as means ± standard errors, and the level of statistical significance was set at $P < 0.05$. Error bars smaller than the symbols do not appear in the figures. The data that significantly differed from WT PLM are indicted with asterisks.

Results

To test the potential impact of PLM phosphorylation on modulating $Ca_V1.2$ channels, the two adjacent phosphorylation sites (S62S63 and S68T69) were replaced with alanine (A) or aspartic acid (D) simultaneously to generate PLM mutants 6263AA, 6869AA, 6263DD and 6869DD. The four potential phosphorylation sites were also replaced with A or D to generate PLM mutants AAAA or DDDD to assess if AAAA or DDDD mutants would further enhance the effects of AA or DD mutants. Whole-cell recordings results showed that WT human and WT canine PLM [8, 9] had similar impacts on the $Ca_V1.2$ channels (Fig. S1), and the amino acids substitution at potential phosphorylation sites did not negate the ability of PLM to modulate $Ca_V1.2$ channels gating (Figs S2–S6, Table S2).

Aspartic acid substitutions increase the peak of the current density (I_{peak})

Whole-cell recording results showed that aspartic acid substitution of phosphorylation sites increased I_{peak} (Fig. 1D–F), while alanine substitution decreased it (Fig. 1A–C). The impact of AAAA and DDDD mutant was more pronounced than that of AA or DD, respectively. Western blot results demonstrated that the expression levels of WT, mutant PLMs and $Ca_V1.2$ channels were similar among various mutant groups (Fig. S7), thus, I_{peak} changes might not be induced by changes on the expression levels of WT, mutant PLMs and $Ca_V1.2$ channels.

Phosphorylation sites mutation mediates the effects of PLM on $Ca_V1.2$ channels gating

To investigate whether PLM phosphorylation status is a crucial determinant of $Ca_V1.2$ gating, the normalized currents were superimposed and compared. As shown in Figure 2, among the four double mutations, 6263AA most noticeably slowed the channel activation (Fig. 2A) and 6869DD most noticeably accelerated the channel VDI (Fig. 2E). AAAA further enhanced the effects of 6263AA on the activation slowdown (Fig. 2C), and DDDD accelerated VDI more than 6869DD (Fig. 2F). Compared with WT PLM, 6869AA and 6263DD did not change the normalized currents visually (Fig. 2B and D), but the quantitative analysis showed that they did affect the gating properties of $Ca_V1.2$ channels (see below). Thus, the PLM-induced $Ca_V1.2$ channels gating changes might be mediated by the amino acid substitutions at the phosphorylation sites.

Phosphorylation sites mutation at S62S63 affects PLM-induced slowing of $Ca_V1.2$ activation

The activation speed was quantified by measuring the time required for the current to increase from 10% to 90% of the peak current ($T_{10\text{-}90}$) [9]. $T_{10\text{-}90}$ was plotted against step voltages to compare differences between PLM mutants and WT PLM. Compared with those of WT PLM, $T_{10\text{-}90}$ values for 6263AA (Fig. 3A) and AAAA (Fig. 3C) increased significantly at hyperpolarized voltages (close to the channel activation threshold), while $T_{10\text{-}90}$ values for 6263DD and DDDD decreased

Journal of Cellular and Molecular Medicine published by John Wiley & Sons Ltd and Foundation for Cellular and Molecular Medicine.

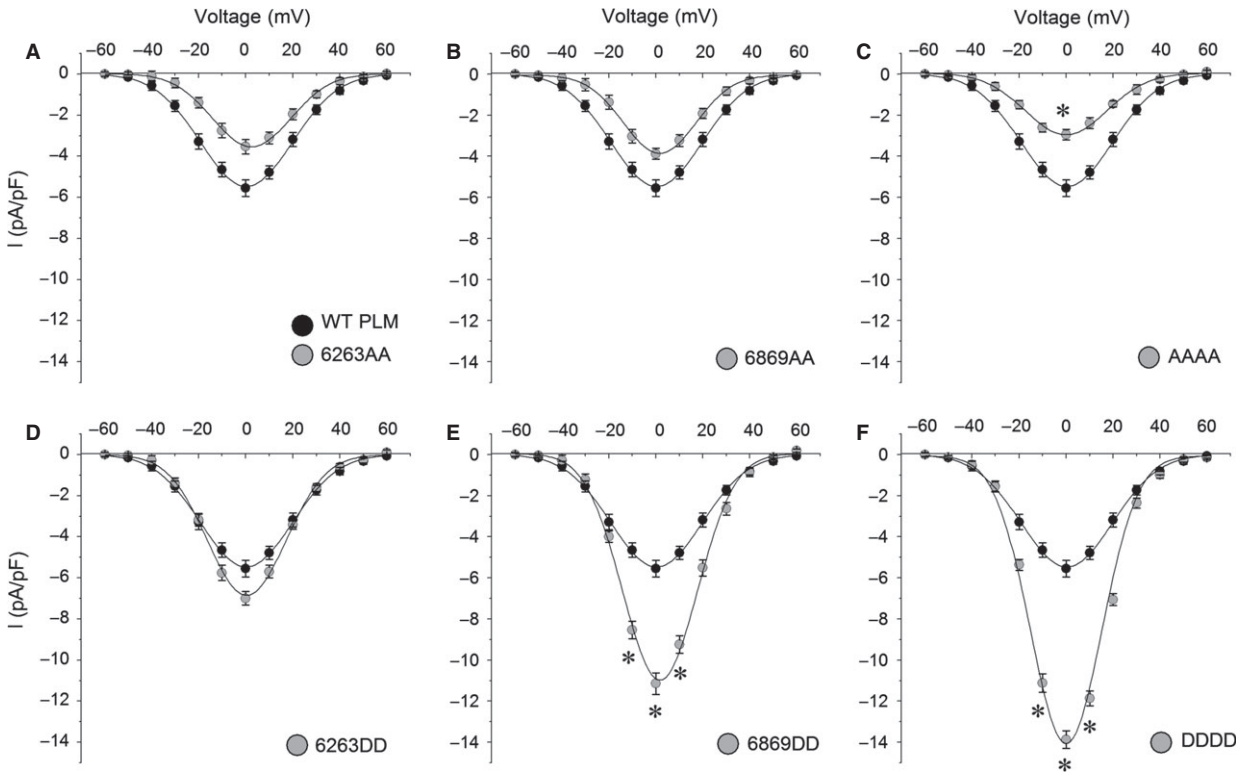

Fig. 1 Aspartic acid substitutions within the phosphorylation sites of PLM increase the peak current density. The current-voltage relationship showing the peak current density (I_{peak}) was recorded from cells with WT and mutant PLMs (n = 6–10). I_{peak} was dramatically increased by PLM phosphomimetic mutants 6263DD, 6869DD, and DDDD and was significantly decreased by the mutant of AAAA, in which the phosphorylation sites were all blocked. * $P < 0.05$ *versus* WT PLM. Ba^{2+} was used as the charge carrier.

significantly at potentials of −20 mV to 0 mV (Fig. 3D and F). $T_{10\text{-}90}$ values for 6869AA slightly increased (Fig. 3B), while $T_{10\text{-}90}$ values for 6869DD slightly decreased (Fig. 3E) at all observed potentials.

Phosphorylation sites mutation at S68T69 affects PLM-induced increase in VDI

To investigate the inactivation gating, we measured the fraction of the current remaining at the end of 300-ms steps (R_{300}) ranging from −20 to +20 mV [9]. R_{300} plot *versus* voltages from $Ca_V1.2$ currents in the presence of 6869DD showed that this mutant significantly enhanced the ability of PLM to increase VDI, and R_{300} values for 6869DD were significantly smaller than those for WT PLM at all observed voltages (Fig. 4E). As expected, DDDD further accelerated PLM-induced increase in VDI, and R_{300} values for DDDD were smaller than those for 6869DD (Fig. 4F). R_{300} values for 6869AA were greater than those for WT PLM (Fig. 4B). Compared with WT PLM, 6263AA slowed VDI (Fig. 4A). AAAA abrogated the PLM-induced increase in VDI, and R_{300} values for AAAA were significantly greater than those for WT PLM at all observed voltages (Fig. 4C). The plot of R_{300} for 6263DD was higher than that for WT PLM, and R_{300} values for 6263DD were slightly larger than those for WT PLM (Fig. 4D).

Only AAAA mutant enhanced PLM-induced slowing of deactivation

Tail currents were evoked by repolarizing to −50 mV following 100-ms depolarizing steps ranging from −20 to +80 mV. The currents at +80 mV were normalized and superimposed to highlight the effects of PLM mutants comparing the effects of WT PLM on the time course of deactivation. All mutant PLMs except AAAA mutant suppressed PLM-induced deactivation slowdown (Fig. 5A–F). These effects were quantified by measuring the relative tail current amplitude at 1 msec. after the peak tail current ($R_{1.0}$) [9]. These isochronic measurements of deactivation were illustrated by $R_{1.0}$ plots *versus* step voltages (Fig. 6). $R_{1.0}$ values for AAAA tended to be larger than those for WT PLM ($P > 0.05$, Fig. 6C). $R_{1.0}$ values for DDDD were significantly smaller than those for WT PLM at voltages ranging from 0 to +80 mV (Fig. 6F). $R_{1.0}$ values for 6869AA were significantly smaller than those for WT PLM at voltages ranging from +50 to +80 mV (Fig. 6B). $R_{1.0}$ values for 6263AA were significantly smaller than those for WT PLM at voltages ranging from +60 to +80 mV (Fig. 6A). $R_{1.0}$-voltage relationship for 6869DD was similar as that of WT PLM (Fig. 6E). $R_{1.0}$ values for 6263DD tended to be smaller compared with those for WT PLM ($P > 0.05$, Fig. 6D).

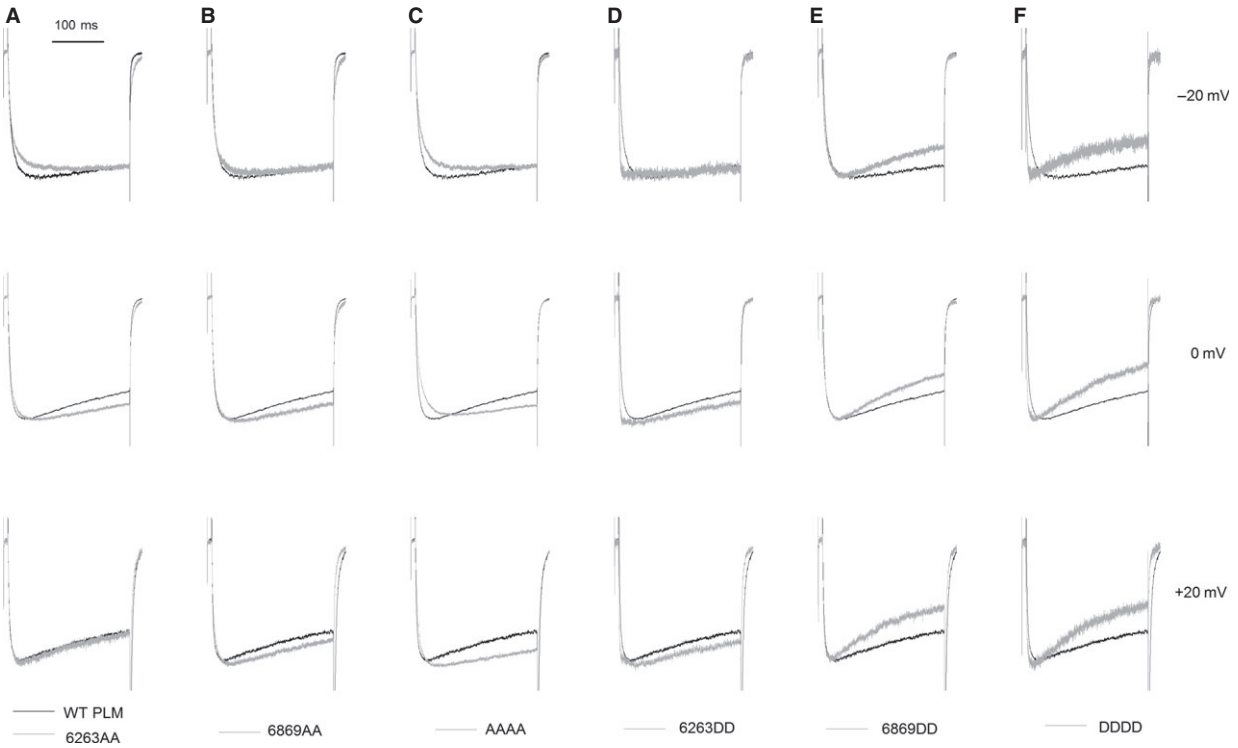

Fig. 2 Amino acid substitutions at the PLM phosphorylation sites alter the $Ca_V1.2$ channel gating kinetics. (**A**–**F**) Whole-cell $Ca_V1.2$ currents recorded with WT PLM (black line) or mutant PLMs (grey line) were evoked by 300-msec. depolarizing steps from a holding potential of −90 mV to the voltages indicated on the right. The currents from 6 to 10 cells were normalized and averaged. Ba^{2+} was used as the charge carrier.

Discussion

The major findings of this study are: (*i*) PLM phosphomimetic mutants 6263DD, 6869DD and DDDD increased while nonphosphorylatable PLM mutants 6263AA, 6869AA, AAAA decreased the peak of $Ca_V1.2$ current density; (*ii*) 6263DD suppressed while 6263AA enhanced PLM-induced activation slowdown; (*iii*) 6869DD enhanced PLM-induced increased VDI, while 6869AA had the same effect on VDI as WT PLM; and (*iv*) only the AAAA mutant enhanced PLM-induced slowing of channel deactivation. Thus, the phosphorylation sites in PLM are important for fine-tuning the gating kinetics of $Ca_V1.2$ channels and could be involved in the kinase-dependent regulation of these channels.

PLM phosphomimetic mutants stimulated LTCCs

Aspartic acid was used to substitute these potential phosphorylation sites in human PLM, as commonly performed [20–23]. Compared with WT PLM, all of phosphomimetic PLM mutants, 6263DD, 6869DD and DDDD, increased the current amplitude, although Western blot analysis indicated that the expression level of $Ca_V1.2$ channels remained unchanged (Fig. S7). PLM is a single transmembrane-spanning protein that inserts into the sarcolemma. Based on nuclear magnetic resonance spectroscopic studies, the purified PLM consists of four α-helices, and the forth helix, H4 (residues 60–68) in the C-terminus, is connected to the third helix, H3 (residues 39–45), by a flexible linker [24, 25]. The forth helix is supposed to orientate with the negatively charged phospholipids of the membrane [24]. We speculate that when PLM is phosphorylated at the phosphorylation sites, the orientation of the cytoplasmic tail might shift and then unlock the connection of PLM and $Ca_V1.2$ channels. This speculation is supported by the fact that $Ca_V1.2$ activation was significantly increased by 6263DD and DDDD (Fig. 3D and F). To confirm the mechanism, additional experiments are warranted, such as Glutathione S-transferase pull-down experiments to examine the exact connection sites between PLM and $Ca_V1.2$ channel.

The phosphomimetic mutation at S62S63 and S68T69 mediates PLM-induced $Ca_V1.2$ channel activation and inactivation, respectively

We observed that 6263AA slowed the channel activation and inactivation more than WT PLM at voltages of −20 mV and −10 mV (Figs 3A and 4A). As channel inactivation could impact the

Journal of Cellular and Molecular Medicine published by John Wiley & Sons Ltd and Foundation for Cellular and Molecular Medicine.

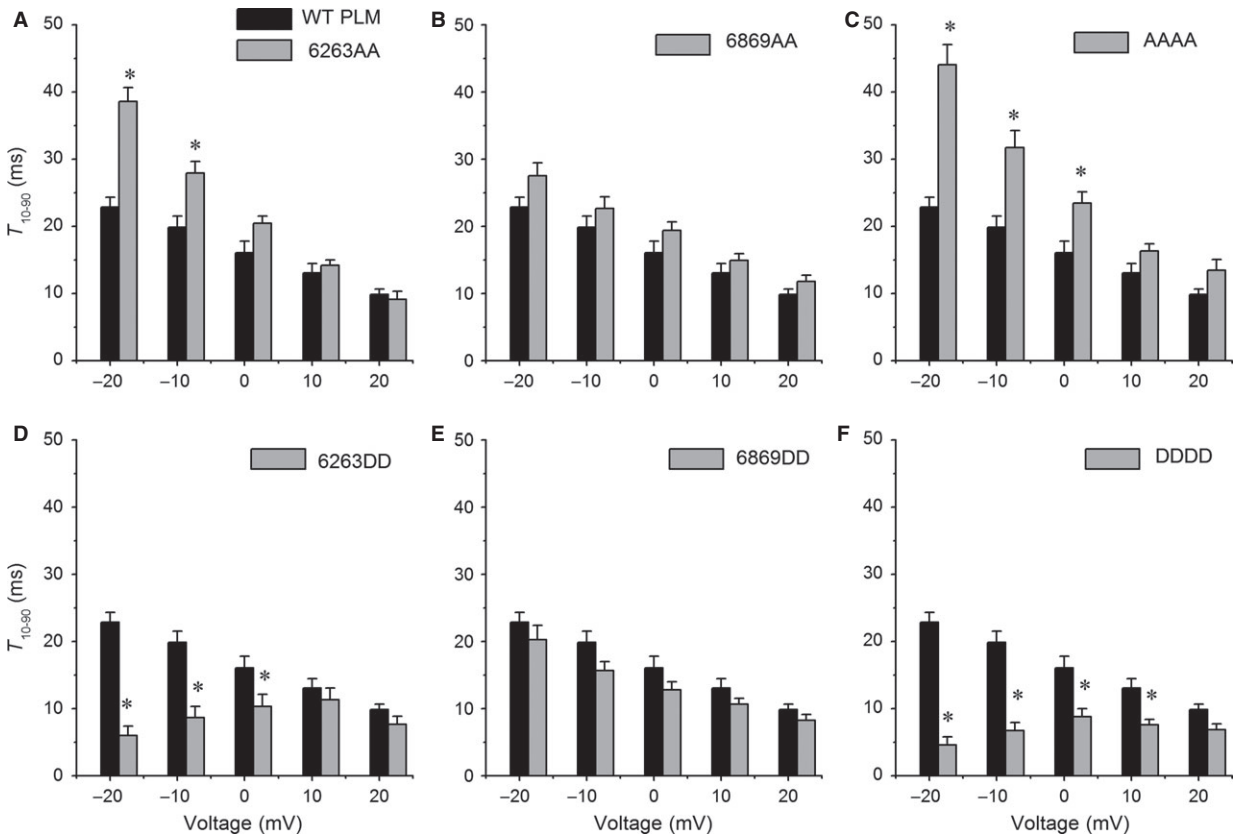

Fig. 3 S62S63 phosphorylation affects the PLM-induced $Ca_V1.2$ activation slowdown. T_{10-90}, the time required to activate from 10% to 90% of the peak currents, was measured from the currents elicited during 300-msec. steps ranging from −20 to +20 mV (10-mV increments, representative currents are depicted in Fig. 2). (**A**) T_{10-90} for 6263AA (grey, $n = 7$) was significantly larger than WT PLM (dark, $n = 10$) at −20 and −10 mV, $P < 0.05$. (**B**) T_{10-90} for 6869AA (grey, $n = 6$) was larger than WT PLM without significant differences at any observed voltages, $P > 0.05$. (**C**) T_{10-90} for AAAA (grey, $n = 7$) was significantly larger than WT PLM at −20, −10 and 0 mV, $P < 0.05$. (**D**) T_{10-90} for 6263DD (grey, $n = 8$) was significantly smaller than WT PLM at −20 and 0 mV, $P < 0.05$. (**E**) T_{10-90} for 6869DD (grey, $n = 6$) was smaller than WT PLM, without any significant differences at the observed voltages, $P > 0.05$. (**F**) T_{10-90} for DDDD (grey, $n = 7$) was significantly smaller than WT PLM at −20 to +10 mV, $P < 0.05$. *$P < 0.05$ *versus* WT PLM.

measurement of channel activation kinetics [9, 26], it is possible that the enhanced slowing of $Ca_V1.2$ channel activation by 6263AA is an indirect consequence of the loss of PLM-induced VDI, indicating that 6263AA might not slow activation more than WT PLM, but it only appears to slow activation because VDI is attenuated. It is supported by the effects of AAAA (as they are the same effects as 6263AA) (Figs 3C and 4C), and also supported by the associated enhancement of VDI and speeding of activation by the DDDD mutant (Figs 3F and 4F). However, the impact that 6263DD has on VDI is similar to that of WT PLM (Fig. 4D), but 6263DD abrogates PLM-induced slowed activation (Fig. 3D), suggesting that *phosphomimetic mutation at S62S63* mediates PLM-induced channel activation without affecting inactivation. Accordingly, 6869DD promotes the channel VDI as fast as DDDD (Fig. 4E), but the activation kinetics of $Ca_V1.2$ currents with 6869DD are similar to those of WT PLM (Fig. 3E). Combined with results showing that 6869AA did not alter PLM-induced activation or VDI (Figs 3B and 4B), it appears that *phosphomimetic mutation at* S68T69 mediates PLM-induced VDI without affecting activation.

The phosphomimetic mutations mediate PLM-induced $Ca_V1.2$ channel deactivation

$Ca_V1.2$ channels have been shown to exhibit modal gating behaviour [27, 28], and PLM promotes mode 2 gating [high open probability (P_O)] by enhancing the voltage- and time-dependent slowing of deactivation [8]. Of the six mutants investigated in this study, only the AAAA mutant, which has all four potential phosphorylation sites substituted by alanine, slowed deactivation, similar to WT PLM (Fig 5C and 6C). The other five mutant PLMs prevented PLM-induced slowed deactivation, although the effects of 6263DD and 6869DD did

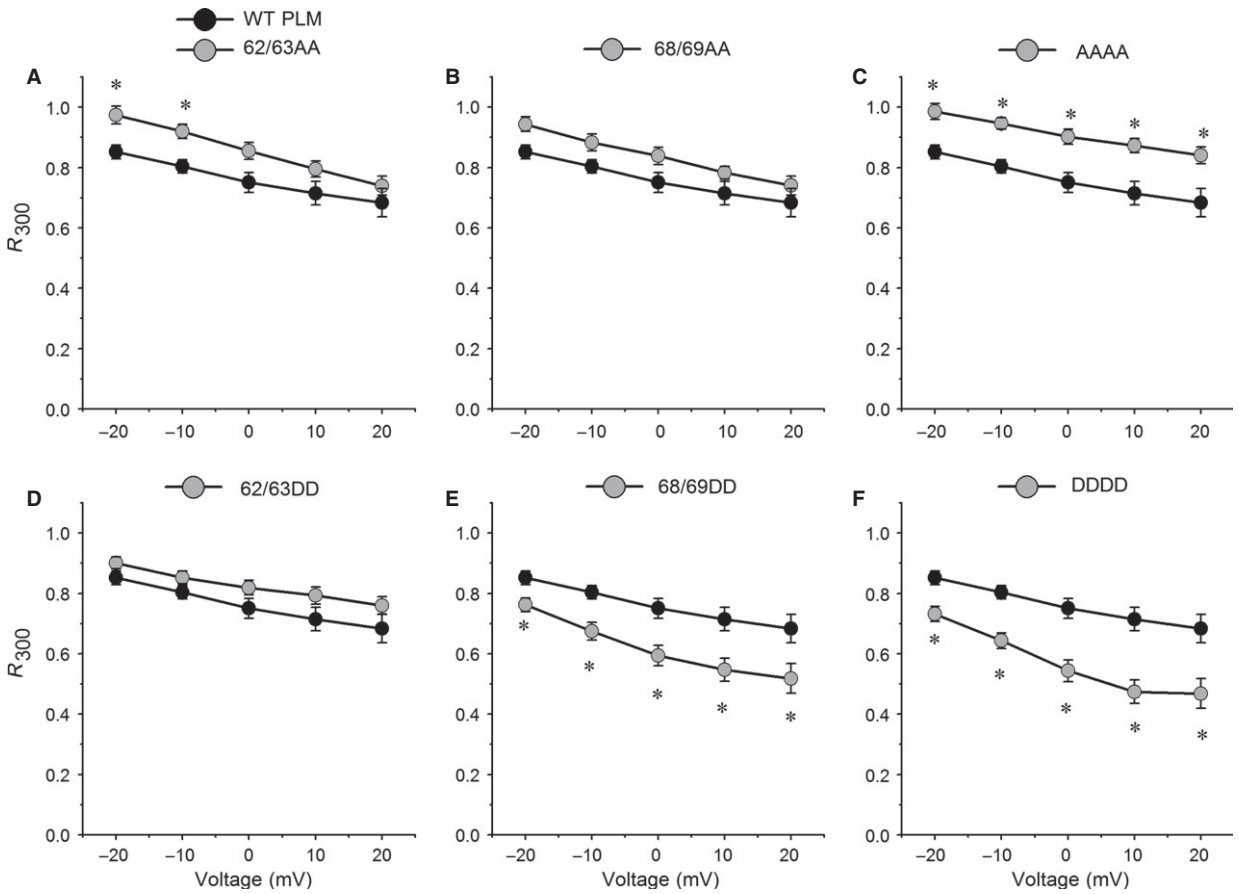

Fig. 4 S68T69 phosphorylation affects PLM-induced increases in voltage-dependent inactivation (VDI). R_{300}, the fraction of peak current measured at the end of 300-msec. voltage steps to the indicated voltages, was plotted *versus* voltage (representative currents are depicted in Fig. 2). (**A**) R_{300} for 6263AA ($n = 7$) was significantly larger than WT PLM ($n = 10$) at −20 and −10 mV, $P < 0.05$. (**B** and **D**) Both of R_{300} for 6869AA ($n = 6$) and 6263DD ($n = 8$) was slightly larger than WT PLM at all observed potentials, $P > 0.05$. (**C**) R_{300} for AAAA ($n = 7$) was significantly larger than WT PLM at all observed potentials, $P < 0.05$. (**E** and **F**) Both of R_{300} for 6869DD ($n = 6$) and DDDD ($n = 7$) was substantially smaller than WT PLM at all observed potentials, $P < 0.05$. *$P < 0.05$ *versus* WT PLM.

not significantly differ from that of WT PLM. As slowed deactivation has been predicted to enhance the relative Ca^{2+} entry during the repolarization phase of the cardiac action potential by favouring the high P_0 state (mode 2), which is arrhythmogenic [8, 13], we speculate that PLM phosphorylation might help protect the Ca^{2+} overload under certain conditions, such as ischaemia. However, it is unclear why 6869AA reduced the PLM-induced slowing deactivation more than 6869DD, thus, single-channel experiments are necessary to confirm the effects of *phosphomimetic mutations* on $Ca_V1.2$ channel mode switching and Ca^{2+} influx.

The changes of $Ca_V1.2$ gating properties mediated by phosphomimetic PLM are not the same as the changes mediated by PKA. For example, PKA-mediated up-regulation of $Ca_V1.2$ activity is dependent on the increase in channel open probability [29], however, the non-phosphorylatable mutant AAAA favoured the high probability. For another example, PKA decreased the VDI *in situ* [30], but the phosphomimetic PLM 6869DD increased the VDI. Zhang, *et al.* showed that phorbol12-myristate13-acetate (PMA, PKC activators) could increase the magnitude of the I_{NCX} in HEK 293 cells expressing NCX alone, however, this effect was much smaller in HEK 293 cells co-expressing NCX and PLM. Thus, the stimulatory effects of PMA on NCX were attenuated by increased PLM phosphorylation [7]. At this point, the direct effect of PKA on LTCC might not be the same as the indirect effect of PKA mediated by PLM and the effect of phosphomimetic PLM on LTCC. Present data were obtained based on the gating properties of $Ca_V1.2$ channels regulated by the phosphomimetic and non-phosphorylatable mutations of PLM. As the effects of PLM mutations on LTCCs modulation were studied in the heterogonous expression systems in HEK 293T cells, the determination of the physiological role of PLM phosphorylation (by PKA or not) and its regulation of LTCCs is beyond the scope of this manuscript and future *in vivo* experiments are warranted to explore the issue. Moreover, the effects of phosphomimetic mutants should be compared with the cAMP-PKA effects on LTCC in intact cardiomyocytes.

Journal of Cellular and Molecular Medicine published by John Wiley & Sons Ltd and Foundation for Cellular and Molecular Medicine.

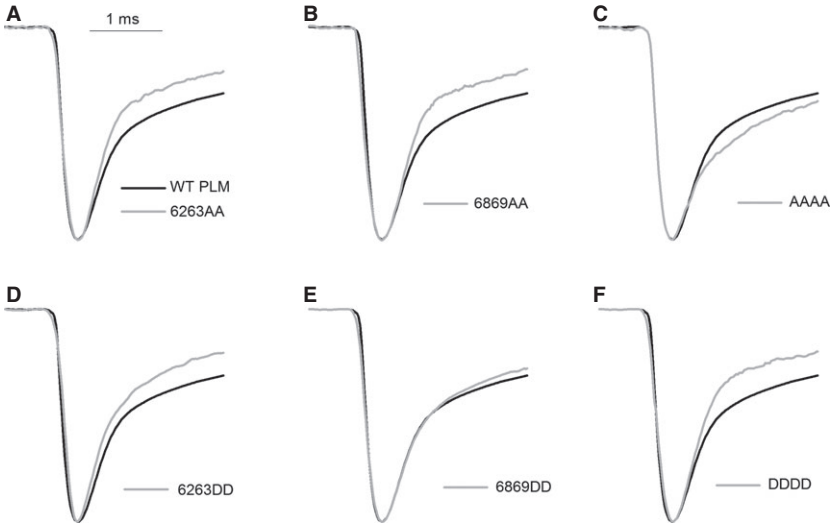

Fig. 5 The mutant of AAAA enhances the PLM-induced slowed deactivation. Sample traces for tail currents with WT PLM (dark line) and mutant PLMs (grey line). (**A**–**F**) Currents were evoked by repolarizing steps to −50 mV following 100-msec. voltage steps to +80 mV. Tail currents from 6 to 10 cells were normalized and averaged. Ba^{2+} was used as the charge carrier.

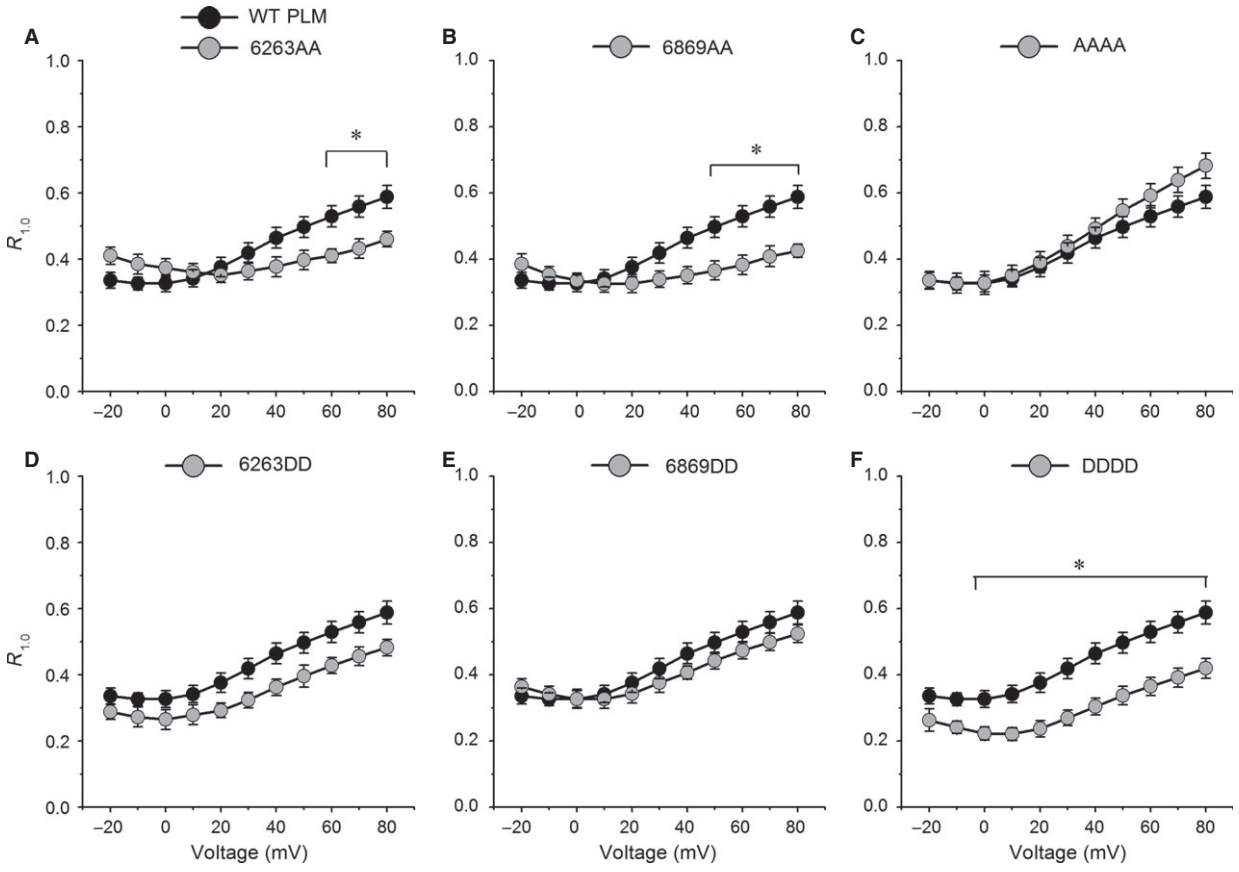

Fig. 6 The mutant of DDDD speeds $Ca_V1.2$ channel deactivation. $R_{1.0}$, the fraction of current remaining 1 msec. after the peak tail current for WT PLM and mutant PLM, was plotted against step voltages (representative currents are depicted in Fig. 5). (**A**) $R_{1.0}$ for 6263AA ($n = 7$) was smaller than WT PLM ($n = 10$) at +60 to +80 mV, $P < 0.05$. (**B**) $R_{1.0}$ for 6869AA ($n = 6$) was smaller than WT PLM at +50 to +80 mV, $P < 0.05$. (**C**) $R_{1.0}$ for AAAA ($n = 7$) was slightly larger than WT PLM, $P > 0.05$. (**D**) $R_{1.0}$ for 6263DD ($n = 8$) was smaller than WT PLM at all observed voltages, but there were no significant differences, $P > 0.05$. (**E**) $R_{1.0}$ for 6869DD ($n = 6$) was comparable to WT PLM, $P > 0.05$. (**F**) $R_{1.0}$ for DDDD ($n = 7$) was smaller than WT PLM at 0 to +80 mV, $P < 0.05$. $*P < 0.05$ *versus* WT PLM.

Physiological relevance of PLM phosphorylation in $Ca_V1.2$ channels gating

It has been shown that changes in $Ca_V1.2$ channels gating, such as impaired VDI, profoundly affect cardiac function [13–16]. TS is a multi-organ disorder caused by a single mutation, G406R (TS mutation), of an alternatively spliced human $Ca_V1.2$ calcium channel containing exon 8a [14]. This TS mutation can lead to lethal arrhythmias, which are thought to be caused by impaired VDI [14, 15]. Our results showed that 6869DD and DDDD could enhance PLM-induced increases in VDI, so we speculate that it is possible that PLM phosphorylation might restore TS-impaired VDI. In fact, LTCC blockers, such as gallopamil, verapamil and diltiazem, can enhance VDI [31, 32] and currently serve as clinically effective medications for certain arrhythmias that result from $Ca_V1.2$ channel-induced early afterdepolarization [33, 34]. Therefore, PLM could be a promising drug target for treating arrhythmias caused by disrupted $I_{Ca(L)}$ inactivation. However, the exact role of PLM phosphorylation in arrhythmias due to LTCCs dysfunction remains largely unclear. For example, the nonphosphorylatable mutants, 6263AA and AAAA, decreased channels activation. It seems that these mutants would prevent excessive Ca^{2+} from entering into cardiac myocytes and reduce the occurrence of arrhythmias. But their effects on activation were not evident at 0 to +20 mV, which is near the action potential peak and early plateau. Additionally, both 6263AA and AAAA abrogated PLM-induced increase in VDI, so the amount of intracellular Ca^{2+} was unknown. Therefore, it would be important to explore the impact of PLM phosphorylation status on $Ca_V1.2$ channels gating in cells, which have undergone hypoxic or mechanical stress conditions *in vitro* and hypoxia and ischaemia situations, or arrhythmia animal models *in vivo*. Such studies may further enhance our understanding on this issue. The present study, however, presented data to show the impact of *phosphomimetic and nonphosphorylatable PLM mutants* on $Ca_V1.2$ channels gating in HEK 293T cells. Future studies are warranted to determine the physiological role of PLM phosphorylation and its regulation of LTCCs in an *in vivo* environment.

In conclusion, our results demonstrate that *phosphomimetic PLM* stimulates LTCCs and alters their dynamics, while PLM nonphosphorylatable mutants lead to opposite effects on LTCCs. Thus, the phosphorylation sites in PLM are important for fine-tuning the gating kinetics of $Ca_V1.2$ channels.

Acknowledgements

We thank Qian Li, Yi-Ping Wang and Po Gao (Department of Physiology, Shanghai Jiaotong University School of Medicine, 280 South Chongqing Road, Shanghai 200025) for the technical assistance. This work was supported by National Natural Science Foundation of China grant (Nos. 81270258 and 81070154 to YG Li), Shanghai City Committee of Science and Technology Research Projects (Nos. 11JC1408200 and 12411951900 to YG Li) and China Postdoctoral Science Foundation grant (No. 2013M530202 to K Guo).

Conflicts of interest

The authors confirm that there are no conflicts of interest.

Author contribution

Conceived and designed the experiments: KG, YPW, YGL; Performed the experiments: KG, YPW, ZWZ, YBJ, WL, XMC; Analyzed the data: KG, ZWZ, YBJ, WL, XMC; Wrote the paper: KG, YPW, YGL; Reviewed, revised and approved the final paper: KG, YPW, ZWZ, YBJ, WL, XMC, YGL.

Supporting information

Additional Supporting Information may be found in the online version of this article:

Figure S1 Effects of WT human PLM on $Ca_V1.2$ channels gating.

Figure S2 Amino acid substitutions at the PLM phosphorylation sites alter $Ca_V1.2$ channel gating kinetics.

Figure S3 S62S63 phosphorylation affects the PLM-induced $Ca_V1.2$ activation slowdown.

Figure S4 S68T69 phosphorylation affects PLM-induced increases in voltage-dependent inactivation (VDI).

Figure S5 The mutant of AAAA enhances the PLM-induced slowed deactivation.

Figure S6 The mutant of DDDD speeds $Ca_V1.2$ channel deactivation.

Figure S7 Amino acid substitutions within the phosphorylation sites of PLM do not alter the $Ca_V1.2$ channel or PLM expression levels.

Data S1 Amino acids substitution at potential phosphorylation sites did not affect the ability of PLM to modulate CaV1.2 channels gating.

References

1. **Sweadner KJ, Rael E.** The FXYD gene family of small ion transport regulators or channels: cDNA sequence, protein signature sequence, and expression. *Genomics*. 2000; 68: 41–56.
2. **Despa S, Bossuyt J, Han F, *et al.*** Phospholemman-phosphorylation mediates the beta-adrenergic effects on Na/K pump function in cardiac myocytes. *Circ Res*. 2005; 97: 252–9.
3. **Silverman B, Fuller W, Eaton P, *et al.*** Serine 68 phosphorylation of phospholemman: acute isoform-specific activation of cardiac Na/K ATPase. *Cardiovasc Res*. 2005; 65: 93–103.

Journal of Cellular and Molecular Medicine published by John Wiley & Sons Ltd and Foundation for Cellular and Molecular Medicine.

4. **Zhang XQ, Moorman JR, Ahlers BA, *et al.*** Phospholemman overexpression inhibits Na^+-K^+-ATPase in adult rat cardiac myocytes: relevance to decreased Na^+ pump activity in postinfarction myocytes. *J Appl Physiol*. 2006; 100: 212–20.
5. **Song J, Zhang XQ, Ahlers BA, *et al.*** Serine 68 of phospholemman is critical in modulation of contractility, $[Ca^{2+}]i$ transients, and Na^+/Ca^{2+} exchange in adult rat cardiac myocytes. *Am J Physiol Heart Circ Physiol*. 2005; 288: H2342–54.
6. **Wang J, Zhang XQ, Ahlers BA, *et al.*** Cytoplasmic tail of phospholemman interacts with the intracellular loop of the cardiac Na^+/Ca^{2+} exchanger. *J Biol Chem*. 2006; 281: 32004–14.
7. **Zhang XQ, Ahlers BA, Tucker AL, *et al.*** Phospholemman inhibition of the cardiac Na^+/Ca^{2+} exchanger. Role of phosphorylation. *J Biol Chem*. 2006; 281: 7784–92.
8. **Wang X, Gao G, Guo K, *et al.*** Phospholemman modulates the gating of cardiac L-type calcium channels. *Biophys J* . 2010; 98: 1149–59.
9. **Guo K, Wang X, Gao G, *et al.*** Amino acid substitutions in the FXYD motif enhance phospholemman-induced modulation of cardiac L-type calcium channels. *Am J Physiol Cell Physiol*. 2010; 299: C1203–11.
10. **Palmer CJ, Scott BT, Jones LR.** Purification and complete sequence determination of the major plasma membrane substrate for cAMP-dependent protein kinase and protein kinase C in myocardium. *J Biol Chem*. 1991; 266: 11126–30.
11. **Presti CF, Jones LR, Lindemann JP.** Isoproterenol-induced phosphorylation of a 15-kilodalton sarcolemmal protein in intact myocardium. *J Biol Chem*. 1985; 260: 3860–7.
12. **Fuller W, Eaton P, Bell JR, *et al.*** Ischemia-induced phosphorylation of phospholemman directly activates rat cardiac Na/K-ATPase. *FASEB J*. 2004; 18: 197–9.
13. **Sicouri S, Timothy KW, Zygmunt AC, *et al.*** Cellular basis for the electrocardiographic and arrhythmic manifestations of Timothy syndrome: effects of ranolazine. *Heart Rhythm*. 2007; 4: 638–47.
14. **Splawski I, Timothy KW, Decher N, *et al.*** Severe arrhythmia disorder caused by cardiac L-type calcium channel mutations. *Proc Natl Acad Sci USA*. 2005; 102: 8089–96.
15. **Barrett CF, Tsien RW.** The Timothy syndrome mutation differentially affects voltage- and calcium-dependent inactivation of CaV1.2 L-type calcium channels. *Proc Natl Acad Sci USA*. 2008; 105: 2157–62.
16. **Yarotskyy V, Gao G, Peterson BZ, *et al.*** The Timothy syndrome mutation of cardiac CaV1.2 (L-type) channels: multiple altered gating mechanisms and pharmacological restoration of inactivation. *J Physiol*. 2009; 587: 551–65.
17. **Wei XY, Perez-Reyes E, Lacerda AE, *et al.*** Heterologous regulation of the cardiac Ca^{2+} channel alpha 1 subunit by skeletal muscle beta and gamma subunits. Implications for the structure of cardiac L-type Ca^{2+} channels. *J Biol Chem*. 1991; 266: 21943–7.
18. **Tomlinson WJ, Stea A, Bourinet E, *et al.*** Functional properties of a neuronal class C L-type calcium channel. *Neuropharmacology*. 1993; 32: 1117–26.
19. **Perez-Reyes E, Castellano A, Kim HS, *et al.*** Cloning and expression of a cardiac/brain beta subunit of the L-type calcium channel. *J Biol Chem*. 1992; 267: 1792–7.
20. **Klimovskaia IM, Young C, Stromme CB, *et al.*** Tousled-like kinases phosphorylate Asf1 to promote histone supply during DNA replication. *Nat Commun*. 2014; 5: 3394.
21. **Tanner SJ, Ariza A, Richard CA, *et al.*** Crystal structure of the essential transcription antiterminator M2-1 protein of human respiratory syncytial virus and implications of its phosphorylation. *Proc Natl Acad Sci USA*. 2014; 111: 1580–5.
22. **DeBerg HA, Blehm BH, Sheung J, *et al.*** Motor domain phosphorylation modulates kinesin-1 transport. *J Biol Chem*. 2013; 288: 32612–21.
23. **Niewiadomski P, Kong JH, Ahrends R, *et al.*** Gli protein activity is controlled by multisite phosphorylation in vertebrate Hedgehog signaling. *Cell Rep*. 2014; 6: 168–81.
24. **Franzin CM, Gong XM, Thai K, *et al.*** NMR of membrane proteins in micelles and bilayers: the FXYD family proteins. *Methods*. 2007; 41: 398–408.
25. **Teriete P, Franzin CM, Choi J, *et al.*** Structure of the Na, K-ATPase regulatory protein FXYD1 in micelles. *Biochemistry*. 2007; 46: 6774–83.
26. **Elmslie KS, Jones SW.** Concentration dependence of neurotransmitter effects on calcium current kinetics in frog sympathetic neurones. *J Physiol*. 1994; 481: 35–46.
27. **Hess P, Lansman JB, Tsien RW.** Different modes of Ca channel gating behaviour favoured by dihydropyridine Ca agonists and antagonists. *Nature*. 1984; 311: 538–44.
28. **Nowycky MC, Fox AP, Tsien RW.** Long-opening mode of gating of neuronal calcium channels and its promotion by the dihydropyridine calcium agonist Bay K 8644. *Proc Natl Acad Sci USA*. 1985; 82: 2178–82.
29. **Yue DT, Herzig S, Marban E.** Beta-adrenergic stimulation of calcium channels occurs by potentiation of high-activity gating modes. *Proc Natl Acad Sci USA*. 1990; 87: 753–7.
30. **Findlay I.** Beta-Adrenergic stimulation modulates Ca^{2+}- and voltage-dependent inactivation of L-type Ca^{2+} channel currents in guinea-pig ventricular myocytes. *J Physiol*. 2002; 541: 741–51.
31. **Motoike HK, Bodi I, Nakayama H, *et al.*** A region in IVS5 of the human cardiac L-type calcium channel is required for the use-dependent block by phenylalkylamines and benzothiazepines. *J Biol Chem*. 1999; 274: 9409–20.
32. **Sokolov S, Timin E, Hering S.** On the role of $Ca(^{2+})$- and voltage-dependent inactivation in Ca(v)1.2 sensitivity for the phenylalkylamine (-)gallopamil. *Circ Res*. 2001; 89: 700–8.
33. **Marban E, Robinson SW, Wier WG.** Mechanisms of arrhythmogenic delayed and early afterdepolarizations in ferret ventricular muscle. *J Clin Invest*. 1986; 78: 1185–92.
34. **Wu Y, MacMillan LB, McNeill RB, *et al.*** CaM kinase augments cardiac L-type Ca^{2+} current: a cellular mechanism for long Q-T arrhythmias. *Am J Physiol*. 1999; 276: H2168–78.